Journal of Experimental Botany, Vol. 57, No. 14, pp. 3601–3618, 2006
doi:10.1093/jxb/erl111 Advance Access publication 12 September, 2006

Journal of Experimental Botany

RESEARCH PAPER

Additional freeze hardiness in wheat acquired by exposure to −3 °C is associated with extensive physiological, morphological, and molecular changes

Eliot M. Herman[1,2,*], Kelsi Rotter[1], Ramaswamy Premakumar[3], G. Elwinger[3], Rino Bae[2], Linda Ehler-King[2], Sixue Chen[4] and David P. Livingston III[3]

[1] *Plant Genetics Research Unit, USDA/ARS, Donald Danforth Plant Science Center, 975 N. Warson Rd, St Louis, MO 63132, USA*

[2] *Climate Stress Laboratory, USDA/ARS, Beltsville, MD 20705, USA*

[3] *USDA/ARS, and North Carolina State University, Raleigh, NC 27695, USA*

[4] *Proteomics Facility, Donald Danforth Plant Science Center, 975 N. Warson Rd, St Louis, MO 63132, USA*

Received 12 June 2006; Accepted 5 July 2006

Abstract

Cold-acclimated plants acquire an additional 3–5 °C increase in freezing tolerance when exposed to −3 °C for 12–18 h before a freezing test (LT_{50}) is applied. The −3 °C treatment replicates soil freezing that can occur in the days or weeks leading to overwintering by freezing-tolerant plants. This additional freezing tolerance is called subzero acclimation (SZA) to differentiate it from cold acclimation (CA) that is acquired at above-freezing temperatures. Using wheat as a model, results have been obtained indicating that SZA is accompanied by changes in physiology, cellular structure, the transcriptome, and the proteome. Using a variety of assays, including DNA arrays, reverse transcription–polymerase chain reaction (RT–PCR), 2D gels with mass spectroscopic identification of proteins, and electron microscopy, changes were observed to occur as a consequence of SZA and the acquisition of added freezing tolerance. In contrast to CA, SZA induced the movement of intracellular water to the extracellular space. Many unknown and stress-related genes were upregulated by SZA including some with obvious roles in SZA. Many genes related to photosynthesis and plastids were downregulated. Changes resulting from SZA often appeared to be a loss of rather than an appearance of new proteins. From a cytological perspective, SZA resulted in alterations of organelle structure including the Golgi. The results indicate that the enhanced freezing tolerance of SZA is correlated with a wide diversity of changes, indicating that the additional freezing tolerance is the result of complex biological processes.

Key words: Aquaporin, cold acclimation, DNA array, electron microscopy, freeze hardiness, proteome, proteomics, transcriptome, wheat.

Introduction

Physiologists and breeders have noted that freezing tolerance beyond that resulting from exposure to low above-freezing temperature is conferred by exposure of plants to temperatures slightly below freezing but before freezing injury occurs (Trunova, 1965; Olien, 1984; Castonguay, 1993, 1995; Livingston, 1996). The acquisition of additional freezing tolerance under these conditions has been called second phase hardening and is here called subzero acclimation (SZA). SZA can provide 3–5 °C of additional freeze tolerance that can provide a critical margin to survive winter. This margin corresponds to approximately one zone on the USDA plant hardiness map of the USA (Cathey and Jordan, 1990) that corresponds to 1–200 km or more of difference in latitude. Similar maps are available for other regions of the world showing the same effect. Because freezing hardiness is one of the primary determinants of plant biogeography, SZA has both agricultural

* To whom correspondence should be addressed. E-mail: eherman@danforthcenter.org
Abbreviations: AFP, antifreeze protein; CA, cold acclimation; NA, non-acclimated; SZA, subzero acclimation.

and ecological implications for plant distribution and crop/cultivar choices.

During cold acclimation (CA) at slightly above-freezing temperatures, a plant adapts physiologically and biochemically, which allows it to survive freezing temperatures. The subject of CA and freezing stress has been reviewed many times (Guy, 1990; Palta and Weiss, 1993; Hughes and Dunn, 1996; Thomashow, 1990, 1999). Recently, much of the emphasis in CA and stress has focused on the identification and function of cold-induced proteins and how the genes that encode these proteins are regulated (Cook *et al*., 2004; Kaplan *et al.*, 2004). With the advent of genomics tools, large-scale assays have been applied to the examination of transcription patterns of CA in several plants. Large-scale transcriptome studies with DNA arrays have shown that CA induces up- as well as downregulation of a very large number of mRNAs (Ndong *et al*., 2001; Fowler and Thomashow, 2002; Ivashuta *et al*., 2002; Seki *et al*., 2002; Fabio *et al*., 2003; Rabbani *et al*., 2003). These assays have shown that diverse plants respond in similar ways by inducing many of the same types of mRNAs such as COR (cold-regulated) proteins and dehydrins. The regulation of many of the genes that are induced by CA is mediated by transcriptional regulators termed CBFs and DREBs (Liu *et al*., 1998). These factors regulate a large number of disparate genes using a common regulatory mechanism (Jaglo-Ottosen *et al*., 1998; Gilmour *et al*., 2000; Vogel *et al*., 2005). The expression of the transcription-regulating proteins at higher temperatures has been shown to confer freezing tolerance when those plants are tested in freeze assays (Kasuga *et al*., 1999).

CA leads to adjustment of protein composition that has been broadly examined as a differential proteomic analysis of NA (non-acclimated) and CA in *Arabidopsis* (Amme *et al*., 2006). Many of the proteins involved in CA can be summarized into two general groups: antifreeze (AFP) and cryoprotective proteins. The AFPs are involved in inhibition of intracellular ice growth and the regulation of ice crystal morphology, while cryoprotective proteins protect intracellular proteins and membranes during the freezing process (Griffith *et al*., 1992, 2005; Sieg *et al*., 1996; Smallwood *et al*., 1999; Tremblay *et al*., 2005). Sieg *et al*. (1996) purified a cryoprotective protein from CA cabbage leaves, and Hincha *et al*. (1997) suggested that these proteins act to protect thylakoid membranes from freeze–thaw damage. Winter rye accumulates six proteins with antifreeze activity, ranging in size from 16 to 35 kDa, in leaf apoplast during CA (Griffith *et al*., 1992; Marentes *et al*., 1993; Hon *et al*., 1994). These proteins are related to pathogenesis-related protein groups, namely, endochitinases, endo-β-1, 3-glucanases, and thaumatin-like proteins (Hon *et al*., 1995). These antifreeze proteins form oligomeric complexes in their native form in various combinations, and it is suggested that these complexes might be more effective in inhibiting ice growth and re-crystallization than individual polypeptides (Yu and Griffith, 1999). The presence of these proteins allegedly explains differences in ice crystal growth in cold-adapted plants compared with controls (Gusta *et al*., 2004; Griffith *et al*., 2005). Apoplastic endochitinase and endo-β-1,3-glucanase, which were induced by pathogens in freezing-sensitive tobacco, did not show antifreeze activity (Hon *et al*., 1995). However, Hincha *et al.* (1997) reported that β-1,3-glucanase from tobacco, which was induced by CA, protected thylakoids against freeze–thaw injury in *in vitro* assays. However, under the same conditions, class I chitinase from tobacco had no effect. These results suggest that antifreeze activity of rye glucanase, chitinase, and thaumatin is not an inherent property of these proteins. It appears that these cold-induced proteins are either isoforms that have antifreeze activity or are post-translationally converted to have antifreeze activity (Thomashow, 1999). Other proteins, such as peach dehydrin (PCA 60) and thaumatin-like protein (AHCSP 33) from peanut, evidently have both antifreeze and cryoprotective activity (Wisniewski, 1997; Dave and Mitra, 1998). In addition, a novel antifreeze protein, with a leucine-rich repeat, has been purified and characterized from carrots (Worrall *et al*., 1998; Smallwood *et al*., 1999).

In contrast to the large body of literature on CA, there is relatively little cellular, biochemical, or molecular research on SZA. Fructan hydrolysis (first described by Trunova, 1965) and a concomitant increase in sugars, particularly in the apoplast, has been reported as a partial explanation for the increase in hardiness during SZA (Olien, 1984; Livingston and Henson, 1998). The increase in molarity of the apoplast solution during SZA due to sugar increases was not high enough to lower the freezing point of the apoplast by more than a fraction of a degree (Livingston and Henson, 1998). However, Canny (1995) demonstrated that the solute concentration in the apoplast is not uniform but that solutes tend to accumulate in discrete regions termed sumps. Livingston *et al*. (2005, 2006*b*) found regions of oat crowns recovering from freezing that appeared to be barriers to freeze damage that could be evidence of the sumps to which Canny (1995) refers. In addition to sugars being distributed unevenly in the apoplast and in separate regions of the crown, the layer of liquid water into which sugars have apparently been released would be very small due to the presence of apoplastic ice at −3 °C (Gusta and Fowler, 1977; Single and Marcellos, 1981; Pearce and Ashworth, 1992). This could lead to regions of considerably higher sugar concentrations in critical tissue within the crown than if the sugars were distributed evenly throughout the apoplast.

Yoshida *et al*. (1997) described a change in the physical state of water in crown tissue of SZA plants that resulted in an increase in water binding strength that is critical for freezing survival of plants. Castonguay *et al*. (1995) reported an increase of raffinose and stachyose in alfalfa

during SZA that may have had a protective effect on plant tissues similar to that proposed for sucrose, glucose, and fructose. To our knowledge, apart from these studies, no information is currently available on the biochemical/biophysical adaptations that may explain the increase in hardiness during SZA. Virtually no information is available on the induction, regulation, and function of genes that may be involved in SZA.

In this study, multiple approaches have been used to investigate the biology of SZA using assays directed to show that physiological changes such as a lowered LT_{50} and changes in water distribution in the crown are correlated with changes in cellular structure, the transcriptome, the proteome, and water channel (aquaporin) expression. The results clearly show that SZA is a complex biological process that has features distinct from CA.

Materials and methods

Plant growth

Wheat (*Triticum aestivum* L. cv. Jackson) seeds were planted in Scotts Metromix 220 (Scotts-Sierra Horticultural Products Co., Marysville, OH, USA) in plastic tubes (2.5 cm diameter×16 cm high) with holes at the bottom for drainage. The tubes were suspended in a grid that held 100 tubes. Plants were treated twice weekly with a modified Hoagland's nutrient solution (Livingston, 1991) and flushed three times weekly with water. Plants were grown for 5 weeks at a day/night temperature regime of 13/10 °C with a 12 h photoperiod in a growth chamber with 240 mmol m^{-2} s^{-1} PAR (80% cool fluorescent and 20% incandescent bulb illumination). These were non-acclimated (NA) plants.

Cold acclimation (CA)

Five weeks after planting, plants were transferred to a chamber at 3 °C with a 12 h photoperiod at 310 mmol m^{-2} s^{-1} for 3 weeks. This 3 week period constituted CA.

To prepare plants for apoplastic extraction and freeze tests, NA and CA plants were removed from tubes and washed free of planting medium in ice water. Roots and leaves of plants were trimmed to allow easier handling; trimming has been shown to have no effect on freezing tolerance of cereal crops (Marshall, 1965; Olien, 1964) and is a routine step in freeze testing winter cereal crops (Mahfoozi *et al*., 2001).

Subzero acclimation (SZA)

CA plants were trimmed and frozen at −3 °C in the dark for 6 h, 1 d, and 3 d to induce SZA. Freeze test equipment did not perform adequately when longer periods at −3 °C were used. Also, longer periods at −3 °C reduced survival in preliminary tests.

Freeze tests

Trimmed, CA plants were placed into slits cut into the sides of doughnut-shaped, cellulose sponges with a pipe in the middle attached to a flange to promote thermal stabilization. Sponges containing plants were placed in plastic bags, sprinkled with shaved ice, and placed into a freezer at −3 °C for the SZA treatments. Three days later, NA and CA plants were trimmed identically to the SZA plants and added to the same freezer in which SZA plants had been placed. Sponges and plants took 6 h to freeze, after which the freezer temperature was lowered 1 °C h^{-1} to the test temperature. Plants were frozen in separate freezers set to −2, −4, −6, −8, −11, −15, −18, and −20 °C. The actual temperature was monitored using thermocouples placed in selected sponges. The freezers were held at these temperatures for 3 h and then gradually warmed to 3 °C at a rate of 2 °C h^{-1}.

When sponges had completely thawed, plants were removed and trimmed of roots to prevent the proliferation of destructive microorganisms (Olien, 1984), and replanted into the same soil mix described above.

Recovering crowns were kept in NA growing conditions for 3 weeks, after which they were rated for survival. Six plants at each temperature were scored either dead or alive in three separate LT_{50} tests for each treatment (NA, CA, and SZA) and analysed using SAS probit analysis (SAS Institute Inc.). Planned comparisons between selected treatments were made using a *t*-test.

Apoplastic fluid extraction

For apoplastic fluid extraction, trimmed plants were reduced to crowns by further cutting roots to 1 cm and shoots to 3 cm. Fifteen NA and CA crowns were centrifuged before freezing. For SZA, crowns from 15 plants were placed in plastic bags, covered with a thin layer of shaved ice to avoid supercooling, and bags were sealed loosely to prevent desiccation. Bags containing crowns were frozen at −3 °C and after 3 d were removed and packed into a cut-off portion of a 50 ml syringe barrel with stems facing towards the Luer tip. A 1 ml high-performance liquid chromatography (HPLC) insert vial was placed at the tip of the syringe barrel to collect apoplastic fluid. The barrel, containing the trimmed crown tissue with the 1 ml vial, was placed in a 50 ml centrifuge tube and centrifuged at 500 *g* for 10 min at 3 °C. This centrifugation process maximized the recuperation of apoplastic fluid while minimizing contamination by cellular solution as indicated by malate dehydrogenase leakage assessment (Livingston and Henson, 1998). This procedure was replicated three times, each time with fresh plant material.

SZA crowns were allowed to thaw for 5 min and pressed gently between paper towels to remove excess water before loading into the syringe cut out. After centrifugation, crowns were placed in an oven at 70 °C for 24 h to determine the percentage of moisture. Percentages were calculated as the weight of liquid extracted (LE) by centrifugation divided by the total weight of water in the plant tissue (LE/fresh weight–dry weight). Experiments were designed as a randomized complete block with three replicates, and analysis of variance as well as Fisher's protected least significant difference (LSD) were calculated using MSTAT (Michigan State University).

Electron microscopy

NA, CA, and SZA crowns were plunge-fixed in ice-cold 4% formaldehyde, 2% glutaraldehyde in 50 mM potassium phosphate buffer, pH 7.4. The fixed material from each condition was post-fixed in 1% (w/v) osmium tetroxide. The samples were dehydrated in a graded ethanol series and embedded in LR white resin. Thin sections were stained with uranyl acetate and lead citrate. Other sections were probed with anti-xyloglycan antibodies and indirectly labelled with anti-rabbit IgG–10 nm colloidal gold as outlined in Yaklich *et al.* (1995). The material was visualized and photographed with a Phillips 300 electron microscope equipped with an axial 1×1 kbit CCD camera (Photometrics). Images were acquired with IP Lab (Scanlytics) and further processed using Adobe Photoshop.

RNA isolation and RT–PCR analysis

Total RNA was isolated from all tissues using the Ambion RNAqueous kit. The amount and concentration of RNA were determined by OD_{260}. For reverse transcription–polymerase chain reaction (RT–PCR), first strand cDNA was synthesized using random primers and the Perkin Elmer Gene Amp RNA PCR kit. cDNA

amplification was done using the Ambion SuperTaq Polymerase kit. Use of the Ambion Quantum RNA classic 18S kit provided internal control of the RNA concentration and PCRs. Ratios of Ambion 18S rRNA primer:competimer were determined empirically. A cycle number of 28–30 rounds for both the specific cDNA and the 18S control was determined to be a linear amplification by removal of reactions after 26, 28, 30, 32, and 34 rounds of amplification. Reactions were run on 1–1.2% agarose gels and stained with ethidium bromide. Band intensity was measured using the Spot Density program from Alpha-Imager. The amplification of the 18S rRNA band was considered not to be affected by the various growing conditions, and therefore the ratio of band intensity between the specific cDNA band and the 18S band was used to control for possible small differences in RNA concentration and amplification between reactions. Specific primers were generated from the C-terminal end and the 3′-untranslated regions of both mRNAs; primers were checked against both the non-redundant and dBEST databases of GenBank to ensure specificity. Wheat PIP-specific primers did not amplify any other clones. PIP1: forward (947–972 bp) CAA TCA GTC TGC CGA CCA TGG ACG G; reverse (1194–1171 bp) CTC CGT TAA ATC GCG TGC GCA GCG G. PIP2: forward (794–820 bp) GCC GCC GTG GCC ACG GTT TAC CAC C; reverse (1059–1029 bp) GGC ACG AGG CCA TCT CTT GCA GTA ACT AGC.

RNA blot analysis: Total RNA was isolated using an RNA isolation kit (Gentra Systems, Minneapolis, MN). A 5 μg aliquot of total RNA was denatured in NorthernMax-Gly load dye (Ambine, Austin, TX, USA) and RNA blot analyses were performed. The blots were probed with PCR-amplified PIP1 and PIP2 products. A 1 μg aliquot of wheat total RNA was used to generate first strand cDNA by using SuperScript II RNase H^- Reverse Transcriptase (Invitrogen, Carlsbad, CA, USA) with an oligo$(dT)_{20}$ primer. A 3 μl aliquot of the first strand cDNA was used for the PCR amplification with *Pfu* DNA polymerase (Stratagene, La Jolla, CA, USA). All SZA samples were amplified using the following conditions: initial denaturation at 95 °C for 2 min, denaturation for 30 s at 95 °C, annealing for 30 s at 55 °C, extension for 1 min at 72 °C, and an additional 10 min extension at 72 °C, 30 cycles. The amplified fragments were isolated and purified from an agarose gel by using a QIAEX II Gel Extraction Kit (QIAGEN, Valencia, CA, USA) and used as probes. For each probe, cDNA was labelled with [α-^{32}P]dCTP using a Random Primed DNA Labeling kit (Applied Biosystems, Foster City, CA, USA) and gel filtered (Edge Gel Filtration Cartridges; Edge BioSystems, Gaithersburg, MD, USA). The analyses were repeated twice to confirm the reproducibility of the results.

The PIP1 (AF366564) fragment was amplified using the primers: forward (PIP1f) 5′-CCGCCATCATCTACAACAAG-3′; and reverse (PIP1r) 5′-GCGCAGCGGTACAATACAGAAG-3′, yielding: CCGCCATCATCTACAACAAGAAGCAGGCGTGGGACGACC-ACTGGATCTTCTGGGTTGGTCCGTTCATCGGTGCGGCGCT-GGCGGCCATCTACCACGTGGTGGTGATCAGGGCCATCCCC-TTCAAGAGCCGCGACTAGTCAGCCAATCAGTCTGCCGACC-ATGGACGGGTGGAATCTTATCGCTGTTCATCGTCGATCGA-TCATGTGGTGGTGGTTGCCCGTGCGTACGTGGCTCATTTC-GCACGCTGTAATTCTCTATCTACCGTCCTCTGTCCCTCTC-CTCGGTGTGTGTGCCTGCCGACAGCGTCACTGTGGCGCAC-CTGTTCAAGTCTGCGAGTTGTGTACTTTCCCTCCCTTCTGT-ATTGTACCGCTGCGC.

The PIP2 (AF366565) fragment was amplified using the primers: forward (PIP2f) 5′-TTCCGGTCCAACTACGA-3′; and reverse (PIP2r) 5′-AGGCCATCTCTTGCAGTAAC-3′, yielding: TTCCG-GTCCAACTACGACGCCTCCGTCTAGCTACTCCCATTCATC-CATCCATTGATGCGTTCCATATCTACTTGTTGATGAGTTG-AGATCCACATTATCGATGGATCTACCGTGTGGCTGTTAAA-ATTGATGGTTAATTAGTATGTTGTTGTGTTACTGAACGTA-TGTATTGCATTGTATGTTAGTGTTGGGTTTACAGTGTTTGC-TAGTTACTGCAAGAGATGGCCT.

DNA arrays

Total RNA was isolated from 100 mg of wheat crown tissue collected from individual plants using the Qiagen RNeasy Plant Mini Kit. DNA was degraded using the Qiagen RNase-Free DNase Set, and an RNA clean up step was performed with the RNeasy MinElute Cleanup Kit.

Hybridization probes for the Affymetrix Barley Genome Array were prepared from this total RNA, as described in Affymetrix protocols. In brief, cDNA was synthesized with SuperScript II reverse transcriptase (Invitrogen) and T7(dT)24 Primer (Operon) and then was purified with the GeneChip Sample Cleanup Module (Affymetrix). The Enzo BioArray HighYield RNA Transcript Labeling Kit (Affymetrix) was used to generate biotin-labelled cRNA targets which were subsequently purified and fragmented with the Genechip Sample Cleanup module.

Targets were transported to the Siteman Cancer Center Gene Chip Facility, Washington University School of Medicine, St Louis, MO, USA where 15 μg of each target was hybridized to an Affymetrix Barley Genome Array which was washed, stained, and scanned on Affymetrix instruments following appropriate Affymetrix protocols. The hybridization cocktail contained control oligonucleotide B2 (Geneset) and control cRNA mix. The control oligonucleotide B2 (5′-biotin: GTCGTCAAGATGCTACCGTTCAGGA-3′) is designed to hybridize to structural features on the chip to allow for proper scanning and grid alignment. The control cRNA mix is provided by the core facility and is composed of a second set of four, biotinylated, *in vitro* antisense transcripts of cDNAs encoding the *Escherichia coli* biotin synthesis genes bioB, bioC, bioD, and the P1 bacteriophage *cre* recombinase gene. Probes corresponding to these bacterial transcripts are also represented on all Affymetrix GeneChips (including test chips). Each synthetic transcript is quantitated and represented at a copy number of 2×10^8–2×10^{10}, corresponding roughly to the expected dynamic range of detection for the GeneChip. This set of control cRNAs allows for the monitoring of hybridization, washing, and staining conditions, and also provides a second set of reference samples for normalizing between experiments (taken directly from the Siteman website).

The chips were washed in the Affymetrix GeneChip Fluidics Station 400 using the 'mini-euk2' program, scanned on the Affymetrix GeneChip array scanner, then image data were captured and converted to numerical output using the Microarray Analysis Suite version 4.0 (taken directly from the Siteman website). These data were deposited in NCBI GEO, series accession number GSE2166.

Expression data were analysed with GeneSpring v7 (Silicon Genetics). Parameters were designated as a function of treatment type, and the value order was set at NA–CA–SZA. Replicates were grouped by treatment type, and the Cross Gene Error Model based on replicates was used for interpretation. Analysis was performed in Log of Ratio Mode. Data were filtered on flags so that only genes scored as present for both replicates of one treatment type were included in the analysis. Data flagged as marginal were considered to be absent.

Isolation of aquaporin clones and other cDNA probes

Library: Wheat crowns were isolated from ice-covered wheat seedlings which had been exposed to 3 weeks of CA at 3 °C followed by 3 d of SZA at −3 °C and immediately frozen in liquid N_2. A non-directional λ ZAP II cDNA library was generated from the frozen tissue by Stratagene as a custom service.

Cloning of wheat PIP2: The cloning was accomplished using a strategy of PCR followed by dilution of positive plaques. The library was plated to a density of ~500 plaques per plate; ~5000 plaques (10 plates) were screened. All plaques from each plate were bulk harvested and subjected to PCR. Pools that amplified a band

similar to that of the control were diluted 1:10 and re-plated to additional plates. Plates were then sectored and all plaques from individual sectors were pooled and screened by PCR. After additional rounds of dilution/PCR, individual plaques were screened by PCR. Positive clones were screened with different primer pairs to confirm specific amplification. One clone, 6-4, was specifically amplified and this clone was sequenced, identified as an aquaporin based on sequence homology, and renamed wPip2. Isolation primers were based on consensus from barley, maize, rice, and sorghum sequences to amplify either most of the cDNA (GG-37 and GG-39) or an internal fragment of ~376 bp (GG-40 and GG-41). Primers were: GG-37, 5′-ATGGAGGG(C/G)AAGGAGGAGGAC; G-39, 5-AGCTTAG(G/C)ACTTGGTCTTGAATG; GG-40, 5′-ACATCATCATGCAGTGCCTGG; GG-41, 5′-GACCCAGAAGATCCAGTGGTC.

PCR was performed under the following conditions: 95 °C 4 min; 35 cycles of 94 °C 45 s, 52 °C 45 s, 72 °C 90 s; 72 °C 10 min; 4 °C hold. The clone was assembled from a double-stranded overlapping sequence.

The cloning of a PIP1(2) aquaporin was a result of a random screen of phagemids derived from the library as part of an expressed sequence tag (EST) project with all clones sequenced using ABI dye-terminator reactions and the ABI device in both directions using T7 or T3 primers. One clone, Wcc302, proved to be a PIP-type aquaporin. All clones were sequenced in multiple directions to confirm the sequence. The final assembled sequences were derived from overlapping consensus sequence from both directions. The complete cDNA sequences for the aquaporins have been deposited in GenBank with accession nos AF366565 for PIP2 and AF366564 for PIP1.

SDS–PAGE and immunoblots

A peptide antibody specific for PIP2 was produced by synthesis of a peptide corresponding to the PIP2 C-terminal (C-QYILRNSAYFRSNYDASV) amino acids with an added N-terminal cysteine residue for coupling to the carrier protein. The peptide was synthesized using an in-house ABI peptide synthesizer. The peptide was coupled to activated haemocyanin (Pierce) and used to elicit antibodies in replicate rabbits. The resulting antiserum was fractionated on a peptide–agarose column produced by reacting the N-terminal cysteine with Pierce sulpholink gel according to the manufacturer's directions. Immunopurified monospecific antibodies were used for immunoblot assays. An antibody directed at the phosphorylated site of the PIP2 was produced by custom synthesis (Biosource International) using the sequence ARKV(pS)LVRAL. Monospecific immunopurified antibodies were used to assay PIP2 phosphorylation.

Total protein from NA, CA, and SZA crowns was obtained by grinding crown tissue in liquid nitrogen in SDS–PAGE sample buffer containing 6 M urea substituting for the glycerol with 5% (v/v) mercaptoethanol. The lysates were heated to 70 °C for 10 min to denature proteins and the lysates were cleared by a 5 min centrifugation in a microfuge. Membrane samples were prepared by grinding 5 g of CA or SZA crowns in cold 20% (w/v) sucrose, 50 mM TRIS–HCl pH 7.4 with a mortar and pestle and centrifuging the lysate in a Beckman J-35 Avanti centrifuge at 10 000 rpm for 10 min. The cleared lysate was loaded into Beckman SW-41 rotor ultracentrifuge tubes and centrifuged for 3 h at 39 000 rpm at 4 °C to obtain total membrane pellets. SDS–PAGE sample buffer with 6 M urea was added directly to the pellets to solubilize, and heated to 70 °C before removing the sample and for analysis by SDS–PAGE immunoblots.

SDS–polyacrylamide gels were run using standard protocols with a 12% uniform resolving gel obtained from BioRad. The fractionated proteins were transferred to PVDF membranes using a BioRad apparatus. The blots were probed with immunoaffinity-purified anti-PIP2 C-terminus or anti-PIP2 phosphopeptide antibodies diluted in TRIS-buffered saline, 5% (w/v) non-fat milk, 0.5% (w/v) Tween-20 by incubating overnight. The blots were washed, probed with anti-rabbit IgG coupled to alkaline phosphatase for 90 min, washed again, and the bound second antibodies visualized with alkaline phosphatase substrate (Sigma). The resulting blots were scanned and the images processed with Photoshop.

Proteomic analysis

Two-dimensional gel electrophoresis and image analysis: Total protein samples were subjected to 2D gel electrophoresis using 2 g of crown tissue. Total protein extract (400 mg) was loaded onto BioRad 11 cm IPG gel strips (pH 3–10 NL) during strip rehydration overnight, after which isoelectric focusing (IEF) was performed for a total of 68 kVh using a Protean IEF Cell (BioRad). Second dimension SDS–polyacrylamide gels (8–16% linear gradient, 8.7×13.3 cm) were run on a BioRad Criterion cell at 60 V for 15 min and then at 180 V for 1 h. Gels were stained with SyproRuby according to the manufacturer's protocols (Molecular Probes, Inc.). Gel images were acquired using a Typhoon laser scanner 9410 (GE Healthcare, USA) and/or a 16-bit cooled CCD camera on a GelPix protein spot excision system (Genetix Ltd, UK). Image analysis was carried out with Phoretix 2D evolution software according to the instruction booklet from Nonlinear Dynamics Ltd (Newcastle, UK). The volume of each spot of interest separated on three replicate gels was normalized against total spot volume, quantified, and excised using the GelPix system.

Protein in-gel digestion and peptide clean-up: Proteins were subjected to in-gel digestion conducted at 37 °C for 10 h in 50 mM NH_4HCO_3 containing 6 μg ml^{-1} modified trypsin (Promega, USA). Peptides were firstly extracted with 1% formic acid/2% acetonitrile and then with 60% acetonitrile. The extractions were combined, lyophilized, and resuspended into 1% formic acid/2% acetonitrile, followed by ZipTip sample clean up according to the manufacturer's instructions.

Protein identification by static nanoESI MS/MS analysis: The protein digests were analysed on an ABI QSTAR XL (Applied Biosystems/MDS Sciex, Foster City, CA, USA) hybrid quadrupole time of flight (QTOF) tandem mass spectrometry (MS/MS) system using a rapid protein identification method. The peptide electrospray tandem mass spectra were processed using Analyst QS software (Applied Biosystems, USA) and searched against the NCBI database and custom databases including Unigene, rice, and wheat using Mascot (version 1.9) with the following constraints: tryptic peptides with up to one missed cleavage site; and 1.0 and 0.1 Da mass tolerances for MS and MS/MS fragment ions, respectively. The charge states of precursor ions selected were 1–3. Oxidation of methionine and carbamidomethylation of cysteine were specified as variable and fixed modifications, respectively. Positive identification was determined by considering the following criteria: (i) number of peptide sequences; (ii) protein sequence coverage; (iii) total Mascot score and individual ion score [a probabilistic implementation of the MOWSE score (http://www.matrixscience.com/help/scoring_help.html)] at P <0.05 to be significant; and (iv) the quality of MS/MS spectra judged essentially by a full-length y-ion series of peptides comprising at least six consecutive amino acids and no missed cleavage. For the protein sequences without functional annotations, the matched sequences were further queried against the NCBI database by BLAST homology and similarity searches.

Results

Additional freezing tolerance resulting from SZA

Exposure of Jackson wheat seedlings to 1 week of CA at 3 °C resulted in a decrease in the LT_{50} by ~4.5 °C beyond

that of NA plants (Table 1). Exposure of CA plants to a temperature of −3 °C for 24 h resulted in an additional, but statistically non-significant decrease in the LT_{50} by 0.4 °C, indicative of possible initial stages of SZA. The LT_{50} of seedlings that had been cold acclimated for a full 3 weeks and then exposed to SZA for 3 d was >2 °C lower.

SZA induces water intracellular displacement to apoplastic space

The volume of apoplastic fluid that was centrifugable from crowns did not change from that of NA plants when they were cold-acclimated and remained at ~10% of the total water content of crowns. When CA plants were exposed to SZA, the volume of centrifugable fluid increased 3-fold (Table 2) and represented >20% of the total water content of crowns.

Crown cells during SZA exhibit changes in ultrastructure compared with CA cells

The ultrastructure of crown cells from SZA plants was compared with that of cells from CA plants in tissue that was conventionally fixed in glutaraldehyde and formaldehyde. Treated plants were rapidly dissected, the crowns divided longitudinally, and the tissue plunge-fixed in fixative on ice. In designing these experiments, the potential for structural modifications occurring prior to stabilization of the structure was considered. Chemical fixation rates are limited by diffusion (which is temperature dependent) into the tissue and the reaction with the target aldehyde-reactive sites. An attempt was made to conduct parallel high-pressure freezing experiments that would provide an alternative method of structural preservation without the limitations of chemical fixation. However, it was found that the preparation of material for high-pressure freezing was more problematic than chemical fixation. In order to high-pressure freeze the tissue, it is necessary to dissect small pieces of the crown on a temperature-equilibrated platform and then load the tissue into temperature-equilibrated planchets. The time needed to set up the material for high-pressure freezing and the manipulations needed with razor blades and working under the microscope with lights that introduce heating proved unsatisfactory due to mechanical damage and thawing of the samples. Conventional fixation by plunging into ice-chilled fixative resulted in tissue that was consistently well fixed by the criteria of organelle morphology and a lack of obvious common electron microscopy artefacts.

Ultrastructural changes during SZA were obvious, primarily in the endomembrane system, with more subtle changes in other organelles. The endoplasmic reticulum (ER) of SZA crown cells often exhibited a more linear morphology, with the lumen of the ER containing electron-dense amorphous deposits (not shown). During CA, Golgi in crown tissue had a typical morphology of five or six closely stacked cisternae assymetrically differentiated from the *cis* to *trans* faces, with small secretion vesicles budding from the *trans* end (Fig. 1A). The five or six stacked Golgi cisternae of SZA crowns appeared to be similar to those in CA tissue, but the *trans* face in SZA samples was often observed, with several attached and adjacent large translucent vesicles giving the appearance of an enlarged vesicle that failed to detach from the Golgi (Fig. 1B, C).

To examine whether these large Golgi-associated vesicles at SZA temperature may have a diagnostic constituent, the distribution of glycans was screened using antibodies and lectins specific for glycosylation status. Among the probes tested were antibodies specific for Golgi fucosyl modification of high mannose side chains, Golgi xyloglycan modification of high mannose side chains, and the lectin concanavalin A for ER origin high mannose. The xyloglycan modification assay provided specificity for the Golgi-associated SZA large vesicles. The xyloglycan antibodies labelled the interior of the large vesicles, which appears to indicate that the vesicular contents were being synthesized by the adjacent Golgi (Fig. 2). The xyloglycan antibodies also labelled the cell wall but not the adjacent vacuole, suggesting that vesicles and their contents are bound for secretion and deposition of the xyloglycan material in the cell wall.

Table 1. *The LT_{50} of Jackson wheat comparing treatments of non-acclimated with cold- and subzero-acclimated (SZA) plants*

Individual LT_{50}s were determined by probit analysis of 48 observations. Numbers in a column followed by the same letter are not significantly different from each other (P=0.05) according to planned comparisons using a t-test. Subzero-acclimated plants had first been cold acclimated for 3 weeks.

Treatment	LT_{50}
Non-acclimated	−7.2 a
Cold acclimated 7 d	−11.8 c
Cold acclimated 7 d, SZA 24 h	−12.2 c
Cold acclimated 21 d	−11.5 c
SZA 1 d	−13.8 e
SZA 3 d	−14.0 e

Table 2. *Apoplastic water centrifuged from wheat crowns under NA, CA, and SZA treatment conditions*

Note that SZA induces a significant increase in apoplastic water. The apoplastic water content data are expressed as a percentage of total crown water. The error range is 3.6% which is the LSD (least significant difference) at a probability level of 0.05. This means that NA and CA are not different from each other but that all three SZA are different from NA and CA but are not statistically different from each other.

NA	4.1%
CA	4.3%
SZA 6 h	10.5%
SZA 1 d	10.9%
SZA 3 d	12.3%

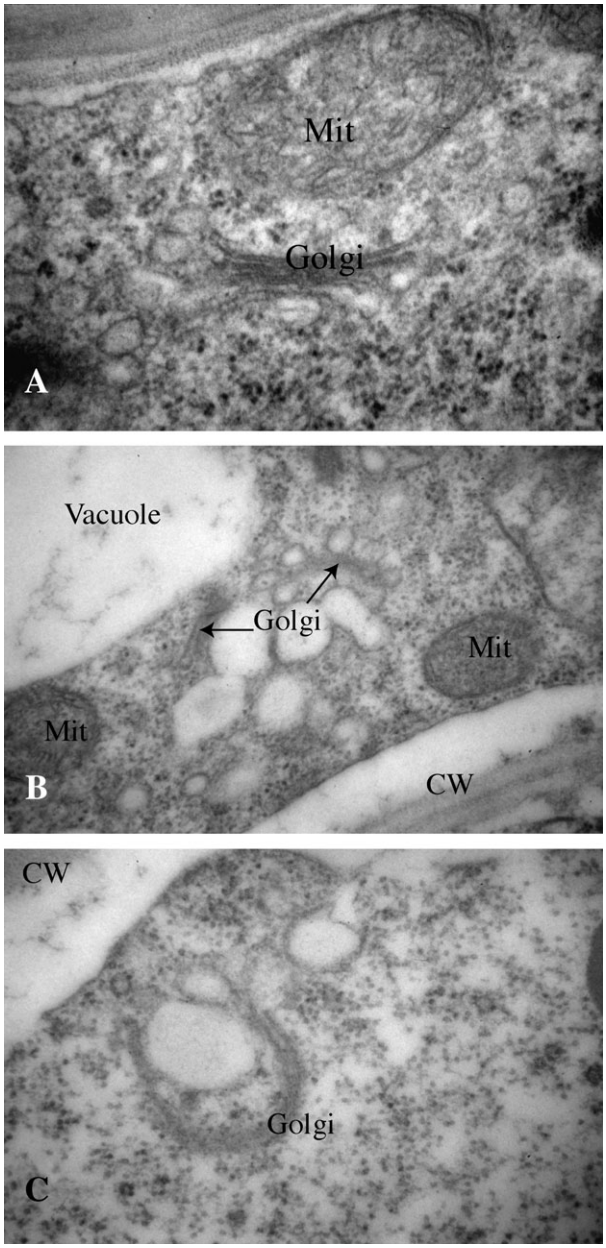

Fig. 1. The morphology of the Golgi is shown comparing CA (A) and SZA (B) treatments on crown tissue from wheat. Under CA, the Golgi morphology is typical of vegetative cells at NA conditions. In contrast, SZA induces morphological changes in the Golgi characterized by the accumulation of large vesicles with an electron-transparent lumen at the *trans* secretion face.

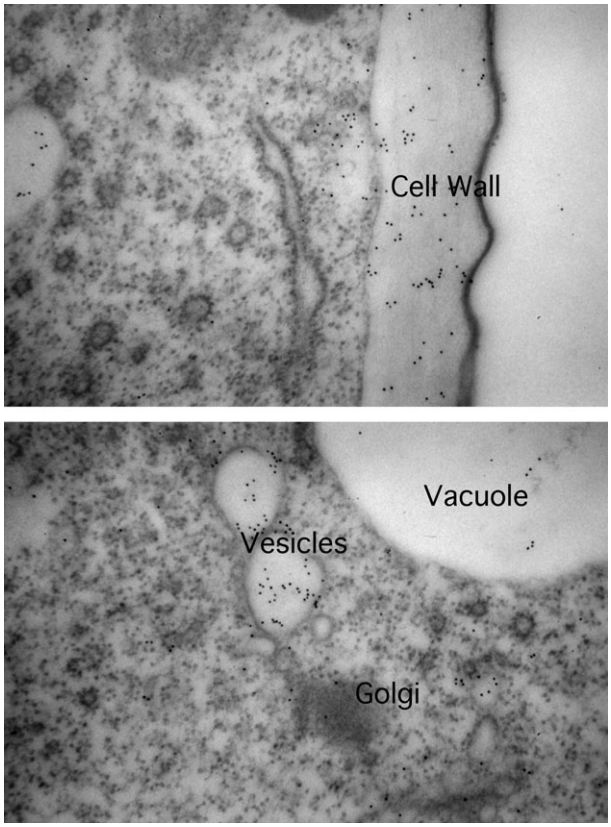

Fig. 2. Anti-N-linked-xyloglycan antibodies label the vesicles accumulated at the *trans*-Golgi under SZA conditions. Note that the SZA Golgi vesicles contain antigens cross-reacting with the anti-xyloglycan antibody. Golgi-derived vesicles are targeted for either extracellular secretion or vacuolar deposition, and the lack of antibody label over the adjacent vacuole in constrast to the cell wall labelling indicates that the SZA Golgi vesicles contain materials destined for extracellular secretion.

Plasma membrane aquaporin is elevated in SZA

Redistribution of water within partially frozen crown tissue (such as during SZA) can be explained thermodynamically as a process whereby equilibrium is re-established between intra- and extracellular spaces by water movement out of cells to regions where ice accumulates. However, a large fraction of water transport and redistribution in plants is facilitated by specific plasma membrane (PIP) and tonoplast membrane (TIP) water pores termed aquaporins (for a review, see Chrispeels and Agre, 1994). Since water transfer during freezing is primarily across the plasma membrane, two distinct PIP isoforms were cloned and sequenced from a cDNA library made from SZA wheat crowns. The two sequences represent examples of the PIP1 and PIP2 (PIP2b) subgroups, with the former correlated with vegetative growth while members of the latter group are often induced in response to abiotic stress such as water deficit (for examples, see Johansson *et al*., 1996; Lee *et al*., 2005). RT–PCR analysis of PIP1 and PIP2 using gene-specific primer pairs indicated that PIP1 expression levels were relatively constant at NA, CA, and SZA (data not shown), while PIP2 expression levels increased from NA to CA and further increased during SZA (Fig. 3A).

The increase in PIP2 abundance was further assayed by immunoblot assay of the protein product of this gene. A specific rabbit antipeptide antibody was elicited using the C-terminal sequence of the PIP2. The resulting antibody labelled a single band in crude protein extracts from wheat crowns fractionated by SDS–PAGE. This band increased

in abundance from NA to CA and remained the same in SZA extracts (Fig. 3B). This pattern was similar to the results obtained with RT–PCR (Fig. 3A), which indicates that CA and SZA induce an increase in abundance of the PIP2 transcript and protein.

PIPs are regulated by phosphorylation (Johansson *et al*., 1996) and chilling (Azad *et al*., 2004; Aroca *et al*., 2005) and are gated to regulate water transfer (Aroca *et al*., 2005; Lee *et al*., 2005). To assess whether there is a difference in phosphorylation status of PIP2 between CA and SZA, SDS–PAGE-fractionated total crown membranes were assayed by immunoblot using an antibody elicited against a phosphorylated peptide derived from the phosphorylation site on the wheat PIP2 sequence (Fig. 3C). The antibody labelled both CA and SZA membranes, with a slightly higher labelling intensity in the SZA membranes. However, the presence of phosphorylated PIP2 in both CA and SZA samples does not support a simple explanation for water export with PIP2 being activated by SZA.

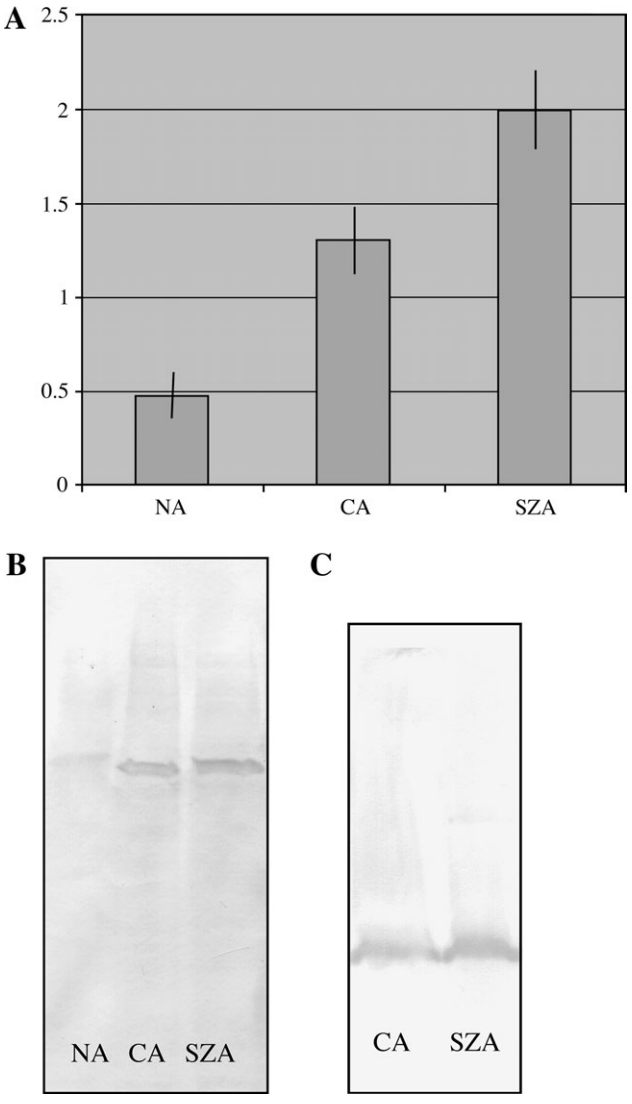

Fig. 3. Changes in PIP2 transcript and correlated protein assays in NA, CA, and SZA are shown. (A) Gene-specific RT–PCR of PIP1 and PIP2b from NA, CA, and SZA crowns, with error bars for the data used to construct the diagram. (B) An immunoblot assay using antibodies specific for the C-terminus of the PIP2b is shown indicating that the PIP2b is present under both CA and SZA. (C) An immunoblot assay is shown of the phosphorylation status of PIP2b in microsomes isolated from CA and SZA crowns. The SZA blots consistently appeared to have a slightly higher specific activity, shown by the labelling intensity.

Northern blot analysis using PCR-amplified PIP1 and PIP2 fragments as probes, that should not be gene specific, indicated that there is a large increase in transcript abundance for PIP1s and PIP2s between NA and CA in crowns and leaf (Fig. 4). Deacclimation for 12 h at 12 °C did not result in any decline in PIP1 and PIP2 transcript abundance (not shown).

DNA arrays show large-scale changes in the transcriptome from CA to SZA

To investigate the transcriptome alteration during SZA, changes in comparative mRNA abundance were assayed using 22 000 element Affymetrix barley arrays. Barley and wheat are close relatives, and the developers of the barley array have shown that it is suitable to assay some wheat messages, obtaining 5500 hits in the spots when probing it with the leaf mRNA population (Close *et al*., 2004). NA, CA, and SZA wheat crowns were used to prepare mRNA samples and probes. These probes were then used to assay replicate 22 000 barley arrays. For analysis of these assays, only positive hits present in both replicates of any one treatment were spot called and the data averaged from each array pair. A total of 5276 spots were called when summing the data for all three conditions. The NA, CA, and SZA plants had 318, 397, and 445 spots present, respectively, that were unique for that treatment. There were 302 spots present in NA/CA but absent from SZA and 227 spots present in CA/SZA but absent from NA. The Venn diagram shown in Fig. 5 illustrates the treatment-specific distribution of the hybridization signals.

Scatter plots of NA/CA and CA/SZA data averaged from replicate arrays with a ±2-fold cut-off shows that the transition from NA to CA and from CA to SZA resulted in changes in the transcriptome pattern (Fig. 6). Differences

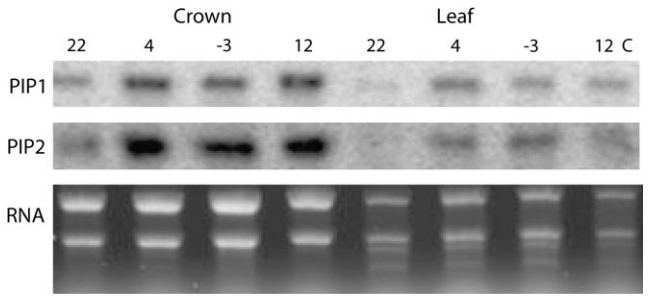

Fig. 4. Shown is a Northern blot analysis of mRNA populations of NA, CA, and SZA, and a 12 h NA recovery from SZA crowns and leaves using probes derived from PIP1 and PIP2 sequences.

between the NA, CA, and SZA sample sets were scored using only those spots present in both array replicates of each treatment, indicating 279 ⩾2-fold upregulated changes between NA and CA and 122 ⩾2-fold upregulated changes between CA and SZA. Of these, 105 and 35 were upregulated from NA to CA and from CA to SZA, respectively. An additional 174 were downregulated ⩾2-fold from NA to CA, and 87 from CA to SZA treatments.

Despite the limited coverage of the 22 000 barley array, even a casual examination of the mRNAs that are up- and downregulated shows that the transition from CA to SZA is complex. The array data showed a wide diversity of messages; selected examples are shown in Table 3 and the full data set is shown Supplementary Table 1 available at *JXB* online, listing the 2-fold up- and downregulated cut-offs. Among the most highly upregulated genes with a ⩾2-fold score were mRNAs encoding a number of putative senescence-related proteins, several cold-regulated proteins and ice recrystallization inhibitors, dehydrins and related late embryogenesis abundant (LEA) proteins, and a diverse set of enzymes and transporters including many that are carbohydrate related. Among the carbohydrate-related upregulated genes are xyloglucan endo-1,4-glucanase, sucrose synthase, β-fructofuranosidase, pyrophosphate-fructose-6-phosphotransferase, 3-glucanase, and glucose-6-phosphate/phosphate translocator. A number of putative and unknown genes included in the array were also upregulated, and many of these have similar homologues in *Arabidopsis*. The 2-fold downregulated genes are similarly diverse and do not exhibit any strong patterns for a group or classes of genes. Among the downregulated genes were genes encoding components of the photosynthetic apparatus or that were plastid localized, along with a diverse set of enzymes and transporters. Many of the upregulated genes were those that would presumably have a function in mitigating the stress of subzero temperature, while those downregulated are indicative of quiescent or a lower level metabolic activity especially for photosynthesis. Some gene expression patterns appear to form pairs, such as upregulation of actin depolymerization protein and downregulation of actin, both indicating a downregulation of the actin cytoskeleton in SZA. Up- and downregulated genes with a two-fold cut-off are available as a online data set (supplementary Table 1 at *JXB* online). Array assay data for NA, CA, and SZA were deposited in NCBI GEO, series accession number GSE2166.

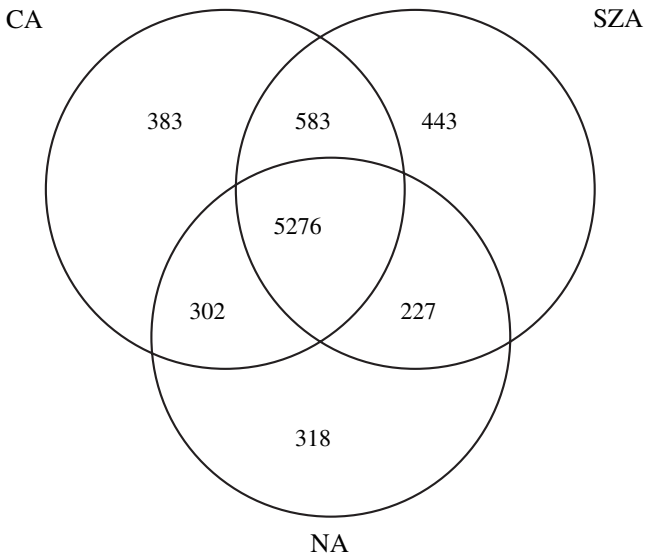

Fig. 5. Shown is a Venn diagram of the spots counted from spots scored present in both replicate arrays for each NA, CA, and SZA treatment. The vast majority of spots that were scored present are found in all three conditions. However, NA, CA, and SZA treatments resulted in spots scored specific for that condition and others that overlap with only the adjacent condition NA+CA or CA+SZA. The Venn diagram illustrates that the barley array identifies numerous genes transcribed, and some of these differentiate between CA and SZA.

Proteome changes

To ascertain whether there was a large-scale remodelling of the protein composition of wheat crowns in the CA–SZA transition, the total proteome was compared using 2D gels.

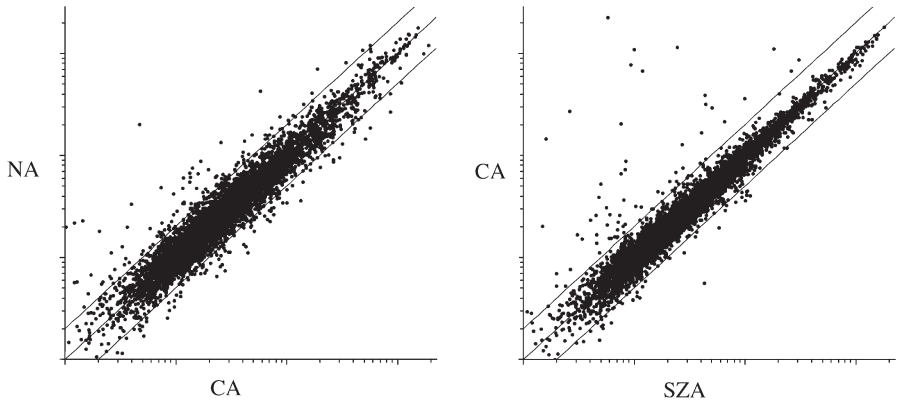

Fig. 6. A scatterplot is shown of expression patterns of NA/CA and CA/SZA transcripts assaying only those present in assays of both replicate 22 000 barley arrays of each treatment. The lines parallel to the centre line mark 2-fold up- or downregulation differences between the two treatments.

Table 3. *Selected transcripts identified from the arrays that are up- or downregulated >2-fold in the CA to SZA transition*

The full data set is available as supplementary information at *JXB* online.

Array gene name	Fold change	Description
Contig5995_at	29.58	Chitinase JC5845
HVSMEa0006I22r2_s_at	20.41	Dehydrin 5 (*Hordeum vulgare*), AAD02262.1
Contig3432_s_at	17.89	High molecular mass early light-inducible protein HV58, chloroplast precursor (ELIP), P14895
Contig4281_s_at	8.37	Cold-regulated protein (*Hordeum vulgare* subsp. *vulgare*), CAC12881.1
Contig1717_s_at	6.591	Dehydrin Dhn5 (*Hordeum vulgare* subsp. *vulgare*), S27761
Contig628_x_at	4.751	Chlorophyll *a/b*-binding protein WCAB precursor (*Triticum aestivum*), AAB18209.1
Contig3670_at	4.688	Ice recrystallization inhibition protein (*Lolium perenne*), CAB87814.1
Contig3776_s_at	4.543	Putative lipid transfer protein [*Oryza sativa* (japonica cultivar group)], AAM74427.1 (AC123594)
Contig4281_at	3.035	Cold-regulated protein (*Hordeum vulgare* subsp. *vulgare*), CAC12881.1
Contig2779_at	2.9	Asparaginyl endopeptidase (*Oryza sativa*), BAA84650.1
Contig6859_at	2.648	Low temperature induced protein (*Hordeum vulgare*), AAC96100.2
Contig4520_at	2.621	Cold acclimation protein WCOR615–wheat (*Triticum aestivum*), T06812
Contig7092_s_at	2.478	Actin depolymerization factor-like protein (*Lophopyrum elongatum*), AAG28460.1
HX10O03r_at	2.432	3-Glucanase (*Sorghum bicolor*), AAL73976.1, AF466201
Contig12134_at	2.295	*cis*-Golgi SNARE protein, putative; protein (*Arabidopsis thaliana*), At2g45200.1
Contig460_s_at	2.256	Sucrose synthase (*Hordeum vulgare*), S24966
Contig21617_at	0.498	Putative peroxidase (*Oryza sativa*), AF172282
ChlorContig14_at	0.491	Photosystem II 43 kDa protein, 1603356H
Contig1815_at	0.461	Photosystem I type III chlorophyll *a/b*-binding protein (*Arabidopsis thaliana*), U01103
Contig2300_s_at	0.461	Chlorophyll *a/b*-binding protein precursor (*Hordeum vulgare*), AAF90200.1
Contig11583_at	0.46	β-Galactosidase precursor (lactase)–garden asparagus, P45582
Contig1389_s_at	0.455	Actin (*Setaria italica*), AAG10041.1
HA28E09r_at	0.454	Photosystem II reaction centre protein K precursor (PSII-K) barley chloroplast, P25877
Contig1529_at	0.442	LHCI-680, photosystem I antenna protein–barley emb (*Hordeum vulgare* subsp.), S52341
HVSMEc0019C19f_at	0.442	Photosystem II protein D1 [*Oryza sativa* (japonica cultivar group)], NP_039360.1
Contig2826_s_at	0.393	DnaJ-like protein (*Oryza sativa*), CAC39071.1
Contig6537_at	0.375	Arabinogalactan protein (AGP16), At2g46330.1
HVSMEb0007O01f_at	0.358	Photosystem II 44 kDa reaction centre protein (P6 protein) (CP43), P10804
HA10A05u_s_at	0.346	Chlorophyll *a/b*-binding protein (*Hordeum vulgare* subsp. *vulgare*), T06193
Contig1888_at	0.345	Light-harvesting complex IIa protein, 1908421A
Contig1604_at	0.344	Oxygen-evolving enhancer protein 2, chloroplast precursor (OEE2), Q00434
HV_CEa0013J19f_at	0.335	Photosystem I P700 apoprotein A1 (*Triticum aestivum*), NP_114259.1
Contig3221_at	0.327	Photosystem I reaction centre subunit, P31093
HVSMEc0011A03f_at	0.325	Photosystem I assembly protein Ycf4 (*Triticum aestivum*), NP_114269.
HVSMEc0016D02f_at	0.305	Photosystem I P700 chlorophyll A apoprotein A1 (PSA), P04966
Contig2764_s_at	0.275	Protochlorophyllide reductase A, chloroplast precursor (PCR A), P13653

Protein differences between NA, CA, and SZA crowns were identified using preparative 2D gels that were stained and analysed using gel scanner software (Fig. 7A–C). Protein spot differences between the gels were identified by visual examination and by computation of spot volume (Figs 7B–D, 8A–C). The transition from NA to CA induced a large number of changes in the spot distribution on 2D gels, which was consistent with previous literature showing that CA results in major changes in transcription and induction of new proteins (Ndong *et al*., 2001; Fowler and Thomashow., 2002; Ivashuta *et al*., 2002; Seki *et al*., 2002; Fabio *et al*., 2003; Rabbani *et al*., 2003). Differences between CA and SZA treatments were much more subtle, with changes of new proteins or proteins lost among the minor proteins on the gel; other changes were in the increasing or decreasing abundance of proteins. Examination of the 2D gels analysed for spot volume resulted in the putative identification of several protein spots that appeared either to increase or to decrease in abundance. Fifty spots that appeared to change between gels were selected and excised with a spot picker. The spots were digested and analysed by nanoelectrospray QTOF MS/MS. The resulting mass spectrum data were analysed and protein identification was obtained by a database search. Several proteins that increased in the CA to SZA transition were identified including 200 kDa cold-induced protein, methyl-binding protein, an unknown protein, abscisic acid-induced protein, universal stress protein, and L7 ribosome protein (Fig. 8A–C). Other proteins that appeared to decrease in abundance included α-tubulin, ATPase synthase α-chain, and ribulose carboxylase large subunit (Fig. 8A–C). A few proteins were induced during the transition from NA to CA but declined during SZA. These included drought-induced protein Sdi-6 and translation factor 5A (Fig. 8A–C).

Discussion

In this study, the physiological processes that support the acquisition of additional freezing tolerance by exposure to 1–3 d of 3 °C below freezing have been investigated by multiple types of assays. Additional freezing tolerance, as measured by LT_{50} assays, was acquired by CA plants after exposure to SZA for 1–3 d. Abrupt changes in temperature do occur quite often in nature, but more typically winter

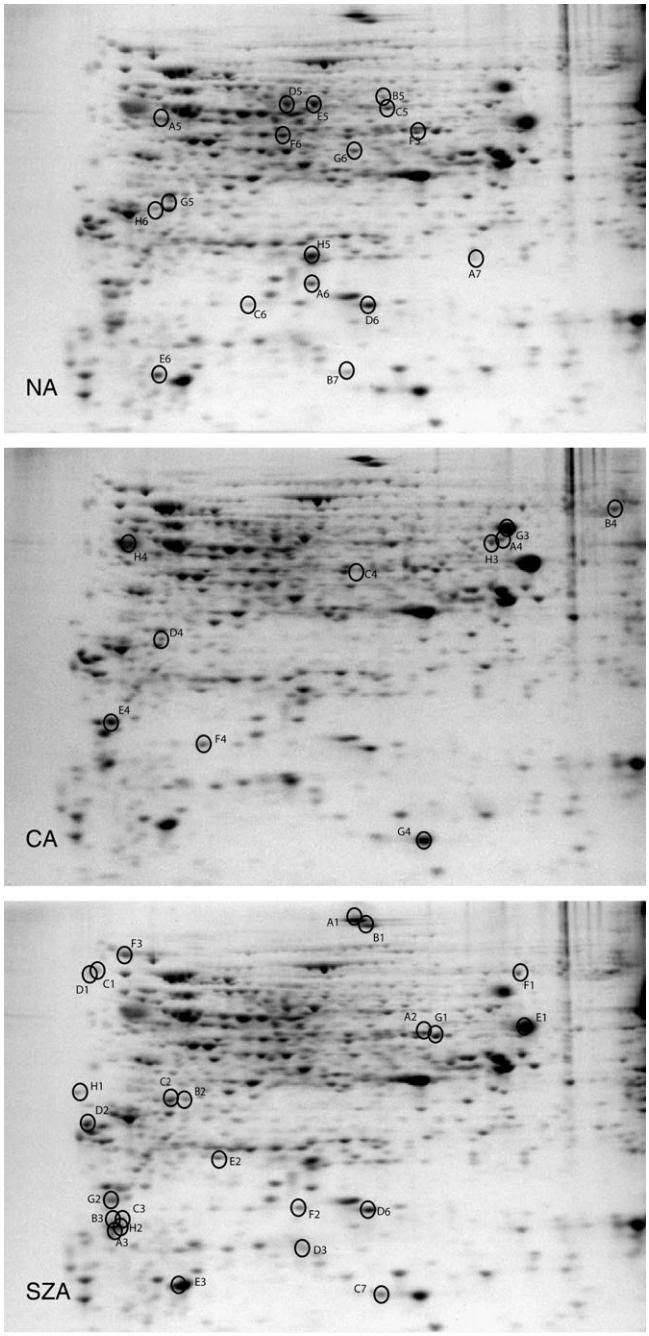

Fig. 7. Two-dimensional gel fractionation of total crown proteins from NA, CA, and SZA treatments. Spots selected for further analysis by mass spectroscopy are circled, with the letter/number code on each spot correlating to the identification and spot volume analysis shown in Fig. 8.

onset is accompanied by a gradual lowering of temperatures from above to below freezing in a diurnal pattern as the season progresses until both day and night temperatures are below 0 °C. As water in the soil freezes, plants will often experience a prolonged period of temperature that is slightly below 0 °C. The additional freezing resistance acquired by SZA is manifested in the biogeography of plants and in the selection of cultivars optimized for winter survival. Plant cold hardiness maps such as the USDA map of North America (Cathey and Jordan, 1990) illustrate that the most significant factor determining the distribution of plants is the lowest temperature plants are expected to encounter during their life cycle. The processes associated with SZA should be a major factor in the biogeography of plants.

The present study investigated whether there are overt biological processes that may explain the additional freezing tolerance acquired by plants exposed to SZA. The extracellular water content of NA and CA plants is essentially identical, indicating that CA does not induce redistribution of water to extracellular spaces. Lowering the temperature to −3 °C induces rapid redistribution of intracellular water to the extracellular space and peaked within 6 h. The formation of ice in the apoplast at −3 °C reduces the chemical potential of water and induces a gradient between liquid intracellular water and ice in extracellular spaces and vessels. This gradient is probably the driving force behind the redistribution of water during SZA, but the rate at which water is redistributed is a result of kinetic factors (Mazur, 1963). Mazur (1963) found that at −2 °C yeast cells which were cooled at 1 °C min^{-1} lost half their water. The amount of water lost in that system depended on the permeability constant for the membrane. While Mazur (1963) did not speculate on the nature of the permeability constant, it is tempting to suggest that this constant may be a function of the effectiveness and regulation of the activity of the PIP population in the membranes (Mazur, 2004). In such a model, the various isoforms and subtypes of PIPs could be independently regulated to provide a wide variation of water translocation activity. The two PIPs examined here are probably only a fraction of the total aquaporin population of wheat. In *Arabidopsis*, 13 PIP genes were identified (Weig *et al*., 1997) so it is likely that with a much larger genome, wheat has many more. The loss of intracellular water in frozen plants concentrates intracellular solutes and would depress the freezing point and prevent desiccation injury of intracellular compartments, as well as restrict formation of intracellular ice. It has now been shown that this water loss is rapid, correlates with the acquisition of freezing tolerance, and that a PIP2 aquaporin and its phosphorylation is induced in parallel. At present, this sequence of events is correlative, and without a null or a knockout of the aquaporin it has not yet been demonstrated that this particular PIP2 aquaporin mediates the water export and the lowering of the LT_{50}. However, the pattern observed supports the suggestion that the acquisition of freezing tolerance during SZA appears to have more than a simple physical basis.

Exposure of wheat plants to SZA results in biological changes in cellular structure as well as transcriptome and proteome content. It is important to note that the 22 000 Affymetrix barley array does not provide complete coverage of the genome and, although barley and wheat are

A

Spot name	Expl. PI/MW	No. pep.	Seq. cov.	EST match	Similar protein	Accession No	3D spot view	Spot volume
A1	6.5/200	2	27		200 kda cold-induced protein	gi|688317	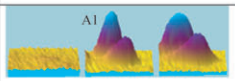	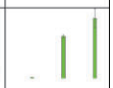
B1	6.6/119				N.I.		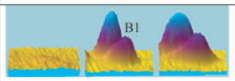	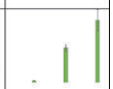
C1	4.1/100	3	17	gi|32775612	methyl binding domain protein	gi|22135477		
D1	4.1/99.7	5	27	gi|32778416	methyl binding domain protein	gi|22135477		
E1	7.9/92.0	6	10		translation elongation factor 1 alpha-subunit	gi|170776	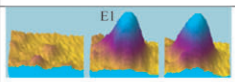	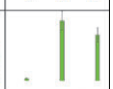
F1	7.9/99.3	30	38		poly(A)-binding protein	gi|1737492	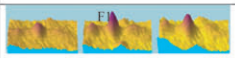	
G1	7.1/80.5	6	10	gi|38994491	Elongation factor 1-gamma	gi|29367381	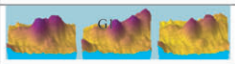	
H1	4.2/54.8	5	32	gi|22211653	Putative abscisic acid-induced protein	gi|28394023		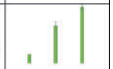
A2	7.0/81.2	5	18	gi|22142502	putative nuclear RNA binding protein	gi|34910712		
B2	5.1/63.0	8	40	gi|14316351	thiamine biosynthetic enzyme	gi|50937969	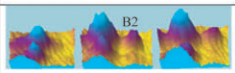	
C2	5.0/62.1	4	15	gi|37208534	OSJNBb0088-C09.11	gi|38605917	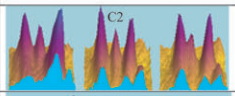	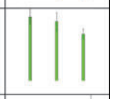
D2	4.2/45.1	8	21	gi|39005920	putative nascent polypeptide	gi|50931251	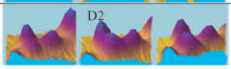	
E2	5.3/44.7	10	47	gi|23072801	putative 20 kDa chaperonin	gi|51090748	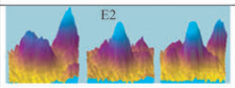	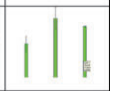
F2	6.1/30.6	10	22	gi|9364677	translation initiation factor	gi|50938957	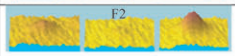	
G2	4.4/32.5	6	29	gi|9883391	drought-induced protein SDi-6	gi|7489327	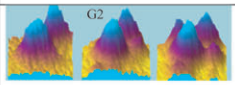	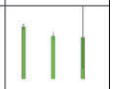
H2	4.4/27.3	7	45		cold acclimation protein WCOR615	gi|7445545	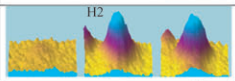	
A3	4.4/26.8	6	21	gi|25427415	OSJNBb0048-E02.12	gi|50924894	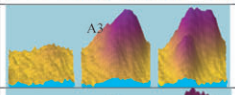	
B3	4.4/27.9	8	42	gi|9609824	cold acclimation protein WCOR615	gi|1657857	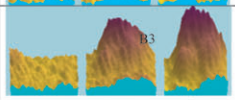	
C3	4.5/28.1	4	24		cold acclimation protein WCOR615	gi|7445545	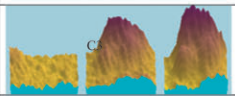	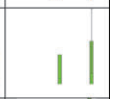
D3	6.1/22.9	4	31	gi|22547657	universal stress protein	gi|50913251	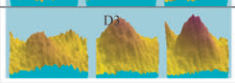	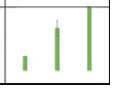

Fig. 8. (*Continued*)

B

E3	5.0/10.2	6	28		glycine-rich RNA-binding protein, low-temperature-responsive	gi|7439979	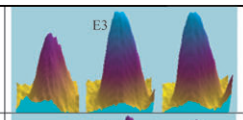
F3	4.6/111	9	53	gi|32683486	hypothetical protein	gi|3753586|	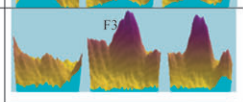
G3	7.8/92.8	5	6		dehydrin 5	gi|33943272	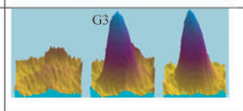
H3	7.7/87.8	7	55	gi|2274988	Hydroxymethyl-transferase	gi|21592544	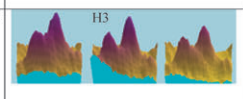
A4	7.7/88.0	6	33	gi|20081598	putative glycine hydroxymethyl-transferase	gi|31126793	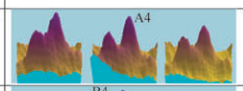
B4	8.8/110	8	31	gi|23086942	SAR DNA binding protein	gi|3288883	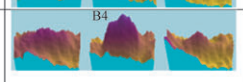
C4	6.6/79.2				N.I.		
D4	4.9/62.8	6	23	gi|37208534	OSJNBb0088-C09.11 [Oryza sativa]	gi|38605917	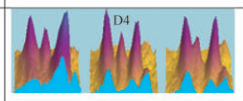
E4	4.5/36.2	15	58	gi|20084481	drought-induced protein SDi-6	gi|7489327	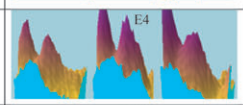
F4	5.3/30.1	3	14	gi|9364677	translation initiation factor 5A	gi|13236654	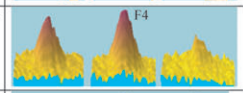
G4	7.1/7.2	4	30	gi|13068084	unknown	gi|13194668	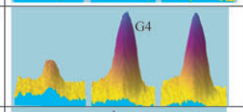
H4	4.5/87.3	9	17		beta-5 tubulin	gi|398849	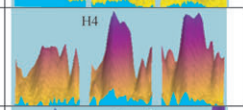
A5	4.9/83.6	24	51		alpha tubulin	gi|1556446	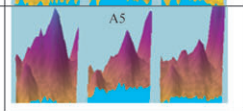
B5	6.7/94.6	24	45		ATP synthase alpha chain	gi|17371040	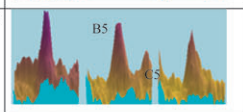
C5	6.8/88.0	18	28		RuBisCO large subunit	gi|132065	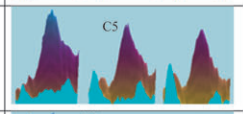
D5	5.9/86.9	7	16	gi|39003570	ATP synthase alpha chain	gi|114419	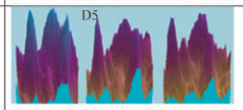
E5	6.1/86.8	15	32	gi|39003570	ATP synthase alpha chain	gi|1430900	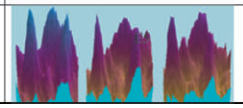

Fig. 8. (*Continued*)

C

F5	6.9/80.9	1	1		translation elongation factor 1-gamma	gi|10444415	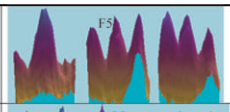
G5	5.0/62.8	9	28	gi|37208534		gi|38605917	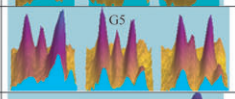
H5	6.2/44.4	18	61		Dehydro-ascorbate reductase	gi|28192421	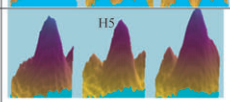
A6	6.1/35.8	14	43	gi|9362847	putative mitochondrial F0 ATP	gi|50946875	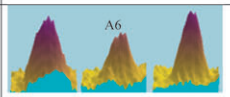
B6	6.6/31.5	3	12	gi|39618495	abscisic acid- and stress-inducible protein	gi|2773154	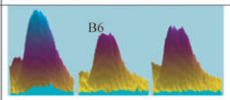
C6	5.6/30.1	6	27	gi|9364677	translation initiation factor	gi|50938957	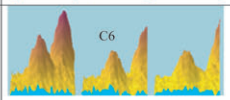
D6	6.7/29.1	1	2	gi|32976952	N.I.		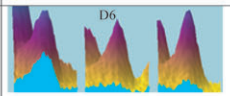
E6	4.8/12.3	7	27		single-stranded nucleic acid binding protein	gi|974605	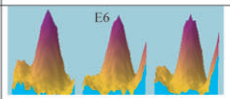
F6	5.9/79.2	7	12		S-adenosyl-methionine synthetase	gi|14600068	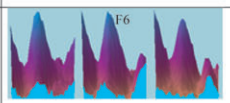
G6	6.5/73.9	3	6		protein disulfide-isomerase precursor	gi|1848212	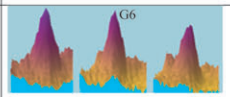
H6	4.8/48.5	8	22		33kDa oxygen evolving protein of photosystem II	gi|21844	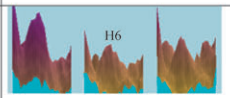
A7	7.6/52.9	2	11		NADH dehydrogenase subunit 9	gi|23495420	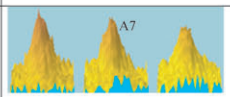
B7	6.4/12.9	8	54		unnamed protein product [Triticum aestivum]	gi|21866	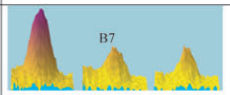
C7	6.7/6.9	2	9	gi|9361719	Ribosomal protein L7Ae-like	gi|21592866	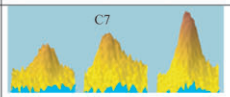

Fig. 8. A chart of the abundance and identification of proteins from 2D gels of crown proteins from NA, CA, and SZA treatments that vary in response to the temperature treatments. The columns of the table show the identification with a specific spot on the 2D gels, the number of peptides and sequence coverage of the mass spectroscopic identification, the identity of the protein from the database search and its match to similar proteins, and the relative abundance of proteins based on spot volume showing both the spot view and calculated spot volume as a histogram. From left to right, the 3D spot views and histograms are from NA, CA, and SZA crowns, respectively.

closely related, it is not known whether the ~6500 present spots on the arrays assayed by the wheat probes are limited by homology or by representation in the mRNA population. Although partial in its representation, the genes identified by the arrays in the up- and downregulated set from CA to SZA resulted in the identification of genes that would be expected to participate in mitigating the stress and assisting in adaptation to subzero temperature. The cold-induced

dehydrins and ice recrystallization inhibition protein genes that are further upregulated in SZA are all obvious candidates for a possible role mitigating freezing stress. The parallel process of water export into the apoplast with the enhanced expression of apoplastic ice recrystallization genes offers the prospect that water trafficking and manipulating ice morphology are linked processes.

The highly induced chitinase gene may be significant; although not an obvious candidate for adaptation to SZA, the cellular damage resulting from SZA can provide a point of entry for attack by snow moulds with the induction of chitinase as one means to impede fungal parasitization (Hiilovaara-Teijo *et al*., 1999). Several of the genes observed as upregulated by the arrays are homologues of genes that encode enzyme activities induced in cold-adapted and stressed plants, for example, chitinase (Hon *et al*., 1995) and glucanase (Hincha *et al*., 1997). Among the other upregulated genes are enzymes involved in possible cell wall modification and several genes otherwise associated with senescence.

The set of genes downregulated during SZA similarly presents a group of genes, many of which can be grouped together by common physiological processes. The plastid and photosynthesis genes, including photosystem I chlorophyll binding and chlorophyll formation, are among the most prominent downregulated genes included in this set. This appears to correlate well with previous observations on the reduction of photosynthesis in CA (Tjus *et al*., 1998; Baldi *et al*., 2001) and appears to continue in SZA. Respiration was reduced in SZA oats to 25% of its value at 3 °C (Livingston *et al*., 2002), plants under SZA conditions give the overt appearance of dormancy, which would require far less photosynthetic capacity than NA or even CA conditions. Other genes downregulated by SZA included actin and kinesin, both important in growing and elongating cells of crown tissue, but probably having more limited roles in the restriction of growth that occurs with SZA. Taken together, the up- and downregulation of genes assayed by DNA arrays indicate that the CA to SZA transition results in key changes in the transcriptome, with cold/dehydration genes being induced and photosynthesis/plastid genes being repressed. Selected examples of these genes are shown in Table 3 with the full set available as supplementary material at *JXB* online. The changes in the transcriptome are consistent with the proposal that there are biological processes underlying the enhancement of freezing tolerance resulting from SZA. The assay of SZA in plants where whole genome arrays are available is likely to disclose many more up- and downregulated genes; with a more comprehensive list, a more complete picture of the processes involved in SZA may emerge.

Overnight exposure of CA plants to SZA resulted in changes in organelle morphology. The Golgi is a sensitive indicator of biological activity due to its rapid turnover. Protein transit through and glycoform processing of proteins in the Golgi has been shown to be rapid, taking at most a few minutes, at least at permissive temperatures. Because the entire structure is undergoing rapid renewal, the CA to SZA changes in Golgi morphology represent an adaptive alteration of Golgi function (Fig. 1B, C). The formation of large vesicles and retention of these vesicles in the near Golgi cytoplasm is a change that undoubtedly resulted from biological rather than purely physical processes. The contents of the enlarged vesicles formed by the Golgi remain uncharacterized; however, by using glycan-specific antibodies, the contents of these vesicles and the cell wall were labelled for complex glycans (Fig. 2A, B), suggesting an ontological relationship. Also, one of the genes detected with the DNA arrays as upregulated by SZA was a homologue of the *Arabidopsis cis*-Golgi SNARE protein. Other changes observed in organelle morphology during SZA included an increased electron-dense lumen of the ER and a nucleoplasm that appeared to have a less dispersed chromatin. Chromatin that is less dispersed may be the beginning stages of nuclear pycnosis found in freeze-damaged cells of orchardgrass (Shibata and Shimata, 1986) and oat (Livingston *et al*., 2005) crowns. Taken together, there are sufficient changes in organelle structure to indicate that SZA induces changes in cellular morphology.

That cell structure is altered during hardening at subzero temperatures is not surprising, because the export of intracellular water would probably require cellular remodelling whether or not this involves reworking existing constituents or adding or removing proteins, lipids, or carbohydrates. The hydrolysis of fructans to simple sugars (Trunova, 1965; Olien, 1984; Livingston *et al*., 1996), during SZA particularly in regions of the crown that are most likely to benefit from acclimation (Livingston *et al*., 2006*a*), should also have cellular implications for the synthesis, transport, and accumulation of carbohydrates. However, cellular remodelling does not differentiate between those changes that occur due to directed programmed changes to prepare for an altered environment and those changes that occur simply as an adaptive response to environmental conditions. The difference is not trivial and is one of the limitations of overt physiology and cell morphology. Changes in morphology are suggestive of changes in the transcription and translation pattern as well as turnover, but morphological changes do not prove this.

The transcriptome and proteomic data presented here represent only a partial data set of the total potential gene and protein changes that may occur during SZA. The DNA array used was of barley sequences, not wheat, and in the present experiments it was found that a little more than 6000 genes (6123 NA, 6588 CA, and 6529 SZA) scored as present out of the 22 000 on the array. The arrays are useful to demonstrate that SZA is accompanied by transcriptome changes, but the choice of genes present on the array coupled with the limitations of cross-species hybridization, even for closely related species, makes the data set only

a partial representation of changes in the total mRNA population. Similarly, the proteome results are limited to relatively abundant proteins of wheat obtained by analysing total crown protein samples. However, even in this data set, proteins increased and decreased during SZA. Follow-up proteomic experiments will need to focus on analysing specific protein subfractions and organelle preparations from specific tissue within the crown (Livingston *et al*., 2005, 2006*a*, *b*). The transcriptome variations suggest that more detailed proteomic data would probably disclose many more examples of protein changes during SZA using concentrated samples from a subset of the total crown protein population.

The present data set indicates that there is a biological basis for the acquisition of added freezing tolerance during SZA with changes in the transcription and translation of specific genes. Determining which of the changes are critical to the acquisition of added freezing resistance will be key to understanding how plants obtain maximum freezing resistance. Understanding and characterizing genes involved in SZA will provide new markers for breeding projects and potentially new targets for gene transfer experiments directed at obtaining the maximum potential freezing tolerance from crop plants.

Supplementary data

Supplementary data can be found at *JXB* online.

References

Amme S, Matros A, Schlesier B, Mock H-P. 2006. Proteome analysis of cold stress response in *Arabidopsis thaliana* using DIGE-technology. *Journal of Experimental Botany* **57,** 1547–1551.

Aroca R, Amodeo G, Fernández-Illescas S, Herman EM, Chaumont F, Chrispeels MJ. 2005. The role of aquaporins and membrane damage in chilling and hydrogen peroxide induced changes in the hydraulic conductance of maize roots. *Plant Physiology* **137,** 341–353.

Azad AK, Sawa Y, Ishikawa T, Shibata H. 2004. Phosphorylation of plasma membrane aquaporin regulates temperature-dependent opening of tulip petals. *Plant and Cell Physiology* **45,** 608–617.

Baldi P, Vale G, Mazzucotelli E, Govoni C, Faccioli P, Stabca AM, Cattevelli L. 2001. The transcript of several components of the protein synthesis machinery are cold-regulated in a chloroplast-dependent manner in barley and wheat. *Journal of Plant Physiology* **158,** 1541–1546

Cathey HM, Jordan R. 1990. *USDA Miscellaneous Publication No. 1475*. Issued January 1990, http://www.usna.usda.gov/Hardzone/ushzmap.html.

Canny MJ. 1995. Apoplastic water and solute movement: new rules for an old space. *Annual Review of Plant Physiology and Plant Molecular Biology* **46,** 215–236.

Castonguay Y, Nadeau P, Laerge S. 1993. Freezing tolerance and alteration of translatable mRNAs in alfalfa hardened at subzero temperatures. *Plant and Cell Physiology* **34,** 31–38.

Castonguay Y, Nadeau P, Lechasseur P, Chouinard L. 1995. Differential accumulation of carbohydrates in alfalfa cultivars of contrasting winter hardiness. *Crop Science* **35,** 509–515.

Chrispeels MJ, Agre P. 1994. Aquaporins: water channel proteins of plants and animals cells. *Trends in Biochemical Science* **19,** 421–425.

Close TJ, Wanamaker S, Caldo RA, Turner SM, Ashlock DA, Dickerson JA, Wing RA, Muehlbauer GJ, Kleinhofs A, Wise RP. 2004. A new resource for cereal genomics: 22K barley GeneChip comes of age. *Plant Physiology* **134,** 960–968.

Cook D, Fowler S, Fiehn O, Thomashow MF. 2004. A prominent role for the CBF cold response pathway in configuring the low-temperature metabolome of Arabidopsis. *Proceedings of the National Academy of Sciences, USA* **101,** 15243–15248.

Dave RS, Mitra RK. 1998. A low temperature induced apoplastic protein isolated from *Arachis hypogaea*. *Phytochemistry* **49,** 2207–2213.

Fábio TSN, De Rosa Jr VE, Menossi M, Ulian EC, Arruda P. 2003. RNA expression profiles and data mining of sugarcane response to low temperature. *Plant Physiology* **132,** 1811–1824.

Fowler S, Thomashow MF. 2002. Arabidopsis transcriptome profiling indicates that multiple regulatory pathways are activated during cold-acclimation in addition to the CBF cold response pathway. *The Plant Cell* **14,** 1675–1690.

Gilmour SJ, Sebolt AM, Salazar MP, Everard JD, Thomashow MF. 2000. Overexpression of the Arabidopsis CBF3 transcriptional activator mimics multiple biochemical changes associated with cold-acclimation. *Plant Physiology* **124,** 1854–1865.

Griffith M, Ala P, Yang DSC, Hon WC, Moffat BA. 1992. Antifreeze protein produced endogenously in winter rye leaves. *Plant Physiology* **100,** 593–596.

Griffith M, Lumb C, Wiseman SB, Wisniewski M, Johnson RW, Marangoni AG. 2005. Antifreeze proteins modify the freezing process *in planta*. *Plant Physiology* **138,** 330–340.

Guy CL. 1990. Cold-acclimation and freezing stress tolerance: role of protein metabolism. *Annual Review of Plant Physiology and Plant Molecular Biology* **41,** 187–223.

Gusta LV, Fowler DB. 1977. Factors affecting the cold survival of winter cereals. *Canadian Journal of Plant Science* **57,** 213–219.

Gusta LV, Wisniewski M, Nesbitt NT, Gusta ML. 2004. The effect of water, sugars, and proteins on the pattern of ice nucleation and propagation in acclimated and nonacclimated canola leaves. *Plant Physiology* **135,** 1642–1653.

Hiilovaara-Teijo M, Hannukkala A, Griffith M, Yu XM, Pihakaski-Maunsbach K. 1999. Snow-mold-induced apoplastic proteins in winter rye lack antifreeze activity. *Plant Physiology* **121,** 665–674.

Hincha DK, Meins Jr F, Schmitt JM. 1997. β-1,3-Glucanase is cryoprotective *in vitro* and is accumulated in leaves during cold accumulation. *Plant Physiology* **114,** 1077–1083.

Hon WC, Griffith M, Chong P, Yang DSC. 1994. Extraction and isolation of antifreeze proteins from winter rye (*Secale cereale* L.) leaves. *Plant Physiology* **104,** 971–980.

Hon WC, Griffith M, Mlynarz A, Kwok YC, Yang DSC. 1995. Antifreeze proteins in winter rye are similar to pathogenesis-related proteins. *Plant Physiology* **109,** 878–889.

Hughes MA, Dunn MA. 1996. The molecular biology of plant acclimation to low temperature. *Journal of Experimental Botany* **47,** 291–305.

Ivashuta S, Uchiyama K, Gau M, Shimamoto Y. 2002. Linear amplification coupled with controlled extension as a means of probe amplification in a cDNA array and gene expression analysis during cold-acclimation in alfalfa (*Medicago sativa* L.). *Journal of Experimental Botany* **53,** 351–359.

Jaglo-Ottosen KR, Gilmour SJ, Zarka DG, Schabenberger O, Thomashow MF. 1998. *Arabidopsis CBF1* overexpression induces *COR* genes and enhances freezing tolerance. *Science* **280,** 104–106.

Johansson I, Larsson C, Ek B, Kjellbom P. 1996. The major integral proteins of spinach leaf plasma membrane are putative aquaporins and are phosphorylated in response to Ca^{2+} and apoplastic water potential. *The Plant Cell* **8,** 1181–1191.

Kaplan F, Kopka J, Haskell DW, Zhao W, Schiller C, Gatzke N, Sung DY, Guy CL. 2004. Exploring the temperature-stress metabolome of Arabidopsis. *Plant Physiology* **136,** 4159–4168.

Kasuga M, Liu Q, Miura S, Yamaguchi-Shinozaki K, Shinozaki K. 1999. Improving plant drought, salt, and freezing tolerance by gene transfer of a single stress-inducible transcription factor. *Nature Biotechnology* **17,** 287–291.

Lee SH, Chung GC, Steudle E. 2005. Gating of aquaporins by low temperature in roots of chilling-sensitive cucumber and chilling-tolerant figleaf gourd. *Journal of Experimental Botany* **56,** 985–995.

Livingston III DP. 1991. Non-structural carbohydrate accumulation in winter oat crowns before and during cold-acclimation. *Crop Science* **31,** 751–755.

Livingston III DP. 1996. The second phase of cold-acclimation: freezing tolerance and fructan isomer changes in winter cereal crowns. *Crop Science* **36,** 1568–1573.

Livingston III DP, Henson CA. 1998. Apoplastic sugars, fructans, fructan exohydrolase and invertase in winter oat: responses to second-phase cold-acclimation. *Plant Physiology* **116,** 403–408.

Livingston III DP, Premakumar R. 2002. Apoplastic carbohydrates do not account for differences in freezing tolerance of two winter oat cultivars that have been second phase cold acclimated. *Cereal Research Communications* **30,** 375–381.

Livingston III DP, Premakumar R, Tallury SP. 2006*a*. Carbohydrate partitioning in crown tissue of oat and rye during cold acclimation and freezing. *Cryobiology* **52,** 200–208.

Livingston III DP, Tallury SP, Owens SA, Livingston JD, Premakumar R. 2006*b*. Freezing in non-acclimated oats: thermal response and histological observations of crowns during recovery. *Canadian Journal of Botany* **84,** 199–210.

Livingston III DP, Tallury SP, Premakumar R, Owens S, Olien CR. 2005. Changes in the histology of cold acclimated oat crowns during recovery from freezing. *Crop Science* **45,** 1545–1558.

Liu X, Kasuga M, Sakuma Y, Abe H, Miura S, Yamaguchi-Shinozaki K, Shinozaki K. 1998. The transcription factors, DREB1 and DREB2, with an EREBP/AP2 DNA binding domain separate two cellular signal transduction pathways in drought- and low-temperature-responsive gene expression, respectively, in Arabidopsis. *The Plant Cell* **10,** 1391–1406.

Mahfoozi S, Limin AE, Fowler DB. 2001. Influence of vernalization and photoperiod responses on cold hardiness in winter cereals. *Crop Science* **41,** 1006–1011.

Marentes E, Griffith M, Mlynarz A, Brush RA. 1993. Proteins accumulate in the apoplast of winter rye during cold-acclimation. *Physiologia Plantarum* **87,** 499–507.

Marshall HG. 1965. A technique of freezing plant crowns to determine the cold resistance of winter oats. *Crop Science* **5,** 83–86.

Mazur P. 1963. Kinetics of water loss from cells at subzero temperatures and the likelihood of intracellular freezing. *Journal of General Physiology* **47,** 347–369.

Mazur P. 2004. Principles of cryobiology. In: Fuller BJ, Lane N, Benson EE, eds. *Life in the frozen state*. Bocan Raton, FL: CRC Press, 4–51.

Ndong C, Dabyluk J, Huner NPA, Sarhan F. 2001. Survey of gene expression in winter rye during changes in growth temperature, irradiance or excitation pressure. *Plant Molecular Biology* **45,** 691–703.

Olien CR. 1964. Freezing processes in the crown of 'Hudson' barley *Hordeum vulgare* (L. emend. Lam.) Hudson. *Crop Science* **4,** 91–95.

Olien CR. 1984. An adaptive response of rye to freezing. *Crop Science* **24,** 51–54.

Palta JP, Weiss L. 1993. Ice formation and freezing injury: an overview on the survival mechanisms and molecular aspects of injury and cold-acclimation in herbaceous plants. In: Li PH, Christersson L, eds. *Advances in plant cold hardiness*. Boca Raton, FL: CRC Press, 143–176.

Pearce RS, Ashworth EN. 1992. Cell shape and localization of ice in leaves of overwintering wheat during frost stress in the field. *Planta* **188,** 324–331.

Provart NJ, Gil P, Chen W, Han B, Chang HS, Wang X, Zhu T. 2003. Gene expression phenotypes of Arabidopsis associated with sensitivity to low temperatures. *Plant Physiology* **132,** 893–906.

Rabbani MA, Maruyama K, Abe H, *et al.* 2003. Plasma membrane aquaporins are involved in winter embolism recovery in walnut tree. *Plant Physiology* **133,** 630–641.

Seki M, Narusaka M, Ishida J, *et al.* 2002. Monitoring the expression profiles of 7000 Arabidopsis genes under drought, cold and high-salinity stresses using a full-length cDNA microarray. *The Plant Journal* **31,** 279–292.

Shibata S, Shimada T. 1986. Anatomical observation of the development of freezing injury in orchardgrass crown. *Journal of Japanese Grassland Science* **32,** 197–204.

Sieg F, Schroder W, Schmitt JM, Hincha DK. 1996. Purification and characterization of a cryoprotective protein (cryoprotectin) from the leaves of cold-acclimated cabbage. *Plant Physiology* **111,** 215–221.

Single WV, Marcellos H. 1981. Ice formation and freezing injury in actively growing cereals. In: Olien CR, Smith MN, eds. *Analysis and improvement of plant cold hardiness*. Boca Raton, FL: CRC Press, 35–59.

Smallwood M, Worrall D, Byass L, Elias L, Ashford D, Doucet CJ, Holt C, Telford J, Lillford P, Bowles DJ. 1999. Isolation and characterization of a novel antifreeze protein from carrot. *Biochemical Journal* **340,** 385–391.

Thomashow MF. 1990. Molecular genetics of cold-acclimation in higher plants. *Advances in Genetics* **28,** 99–131.

Thomashow MF. 1999. Plant cold-acclimation: freezing tolerance, genes and regulatory mechanisms. *Annual Review of Plant Physiology and Plant Molecular Biology* **50,** 571–599.

Tjus SE, Moller BL, Scheller HV. 1998. Photosystem I is an early target of photo inhibition in barley illuminated at chilling temperature. *Plant Physiology* **116,** 755–764.

Tremblay K, Ouellet F, Fournier J, Danyluk J, Sarhan F. 2005. Molecular characterization and origin of novel bipartite cold-regulated recrystallization inhibition proteins from cereals. *Plant and Cell Physiology* **56,** 884–891.

Trunova TI. 1965. Light and temperature systems in the hardening of winter wheat and the significance of oligosaccharides for frost resistance. *Fiziologiya i Biokhimiya Kulturnykh Rastenii* **12,** 70–77.

Vogel JT, Zarka DG, Van Buskirk HA, Fowler SG, Thomashow MF. 2005. Roles of the CBF2 and ZAT12 transcription factors in configuring the low temperature transcriptome of *Arabidopsis*. *The Plant Journal* **41,** 195–211.

Weig A, Deswarte C, Chrispeels MJ. 1997. The major intrinsic protein family of Arabidopsis has 23 members that form three distinct groups with functional aquaporins in each group. *Plant Physiology* **114,** 1347–1357.

Wisniewski M. 1997. Immunolocalization and *in vitro* cryoprotective activity of PCA 60: a peach dehydrin. *Biol. Bull. Poznan* **34** (Suppl), 82.

Worrall D, Elias L, Ashford D, Smallwood M, Sidebottom C, Lillford P, Telford J, Holt C, Bowles D. 1998. A carrot leucine-rich-repeat protein that inhibits ice recrystallization. *Science* **282,** 115–117.

Yaklich R, Herman EM. 1995. Protein storage vacuoles of soybean aleurone cells accumulate a unique glycoprotein as well as proteins thought to be embryo specific. *Plant Science* **107,** 57–67.

Yoshida M, Abe J, Moriyama M, Shimokawa S, Nakamura Y. 1997. Seasonal changes in the physical state of crown water associated with freezing tolerance in winter wheat. *Physiologia Plantarum* **99,** 363–370.

Yu XM, Griffith M. 1999. Antifreeze proteins in winter rye leaves form oligomeric complexes. *Plant Physiology* **119,** 1361–1369.